Vibrational Contributions to Indirect Spin−Spin Coupling Constants Calculated via Variational Anharmonic Approaches

Mikkel B. Hansen,*,† Jacob Kongsted,‡ Daniele Toffoli,†,§ and Ove Christiansen†,§

The Lundbeck Foundation Center for Theoretical Chemistry and Center for Oxygen Microscopy and Imaging, Department of Chemistry, University of Århus, Langelandsgade 140, DK-8000 Århus C, Denmark, and Department of Theoretical Chemistry, Chemical Center, University of Lund, P.O. Box 124, S-221 00 Lund, Sweden

Received: May 15, 2008; Revised Manuscript Received: June 26, 2008

Zero-point vibrational contributions to indirect spin−spin coupling constants for N_2, CO, HF, H_2O, C_2H_2, and CH_4 are calculated via explicitly anharmonic approaches. Thermal averages of indirect spin−spin coupling constants are calculated for the same set of molecules and for C_2X_4, X = H, F, Cl. Potential energy surfaces have been calculated on a grid of points and analytic representations have been obtained by a linear least-squares fit in a direct product polynomial basis. Property surfaces have been represented by a fourth-order Taylor expansion around the equilibrium geometry. The electronic structure calculations employ density functional theory, and vibrational contributions to indirect spin−spin coupling constants are calculated employing vibrational self-consistent-field and vibrational configuration-interaction methods. The performance of vibrational perturbation theory and various approximate variational calculations are discussed. Thermal averages are computed by state-specific and virtual vibrational self-consistent-field methods.

I. Introduction

Nuclear magnetic resonance (NMR) parameters are strongly influenced by variations in the molecular geometry.[1−5] This is perhaps most well-known for spin−spin coupling constants (SSCC) where the empirical Karplus equation is used for modeling the dependence of $^3J_{HH}$ SSCCs on the involved dihedral angle. Other empirical relations exist that describe the geometry dependence of vicinal SSCCs.[6] Therefore, vibrational contributions, i.e., the effect of also treating the dynamics of the nuclear framework and thus not only calculating the property at the equilibrium geometry, to these parameters are expected to be significant. The relative importance of the rotational and vibrational contributions depends on both the nature of the molecular system of interest and also the temperature. For molecules characterized by high vibrational frequencies the rotational contribution may dominate the total ro-vibrational correction at low temperatures.[7] However, for molecules possessing lower vibrational frequencies the vibrational correction usually becomes more important to consider than the rotational counterpart, especially at higher temperatures. In this context a first step in the direction of introducing dynamical effects on the SSCCs would be to consider the zero-point vibrational contribution (ZPVC) to the SSCCs. In addition, since experimental NMR measurements are always performed at finite temperatures, excited vibrational levels become populated (according to the Boltzmann distribution law) and hence the SSCCs are expected to be temperature dependent. Indeed, this has been shown by Wigglesworth et al.[8] and Sauer et al.[9] For flexible molecules, i.e., molecules characterized by several different conformations which are generally not reached by small amplitude vibrations, a proper averaging over the SSCCs derived from different conformations should be employed. However, in this paper we will restrict ourselves to molecular systems dominated by only one conformation with a well defined minimum energy. Vibrational effects are then described as the effect of vibrational motion around this energy minimum.

The calculation of zero-point vibrational contributions (ZPVC) to molecular properties has conventionally been performed using a vibrational perturbation theory (VPT) approach[10−13] which is inherently a nonvariational treatment. Although perturbation theory for vibrational states frequently has revealed itself as a powerful method, it is generally not believed to be as accurate and robust as variational procedure. In this paper, we will therefore use different variational methods for the solution to the vibrational problem as well as the calculation of vibrationally averaged SSCCs. After obtaining very accurate reference values for the ZPVC (within the given electronic structure method) we use these to discuss the accuracy and cost of other approximate schemes including VPT.

According to the formalism of Ramsey,[14] the calculation of indirect spin−spin coupling constants requires the evaluation of four different terms: (i) the Fermi contact (FC) contribution which describes polarization of the spin density at the nuclei due to Fermi coupling (this contribution is usually significant); (ii) the spin dipole (SD) contribution which in a similar manner describes polarization of the spin density resulting from the dipole field of the nuclear moment. The orbital currents induced by the magnetic moments are usually divided into two contributions: (iii) the diamagnetic spin−orbit (DSO) and (iv) paramagnetic spin−orbit (PSO) contributions. The DSO contribution may be evaluated as an expectation value. The FC, SD, and PSO contributions are however found from the linear response function requiring the solution of linear response equations.[1] The calculation of SSCCs is challenging because of the large number of response equations that need to be solved and because

* Corresponding author. E-mail: mbh@chem.au.dk. Phone: +45 89423827. Fax: +45 86196199.

† The Lundbeck Foundation Center for Theoretical Chemistry, Department of Chemistry, University of Århus.

‡ University of Lund.

§ Center for Oxygen Microscopy and Imaging, Department of Chemistry, University of Århus.

10.1021/jp804306s CCC: $40.75
Published on Web 08/15/2008

of the slow convergence of computed SSCCs with increasing basis set size, requiring the use of general large and uncontracted, at least for the s-type functions, basis sets in order to reach the basis set limit.[15,16] The calculation of SSCCs are for some approximate methods, i.e., Hartree−Fock, often complicated by triplet instability problems.[17] Density functional theory (DFT) methods include some electron correlation effects and thus to some extent overcome these problems.[18]

In this paper, we will continue our work on vibrational and thermal effects on molecular properties.[19] Within the present context, we (i) calculate zero-point vibrational contributions to SSCCs using the vibrational self-consistent field (VSCF) and vibrational configuration interaction (VCI) models using explicitly anharmonic potentials and (ii) study the thermal effects on SSCCs within the VSCF framework in combination with statistical mechanics.

We use DFT methods for the electronic structure calculations. Although DFT may lack high predictive power in an absolute sense, it is hoped to have high enough accuracy for the variation of the property to give reasonable vibrational corrections. We note that a DFT study of ZPVC to SSCCs using perturbation theory has been published recently by Ruden et al.[12] In the present work, we consider some of the same molecules and basis sets as in ref 12. Very recently, Hirata et al. showed that vibrational contributions to SSCCs in the FHF^- molecule may be calculated very accurately within the VCI framework.[20]

II. Theory

A. Potential and Property Surfaces. In this section the procedure used for the construction of the Born−Oppenheimer (BO) potential energy and molecular property surfaces will be outlined together with the nomenclature adopted.

Since the large dimensionality of the BO potential (the number of internal degrees of freedom, M) severely hampers an exact solution of the nuclear Schrödinger equation, we adopt a hierarchical representation of the adiabatic potential through a converging sequence of approximate potential terms

$$V^{(1)}, V^{(2)}, V^{(3)}, \ldots, V^{(M)} \tag{1}$$

where the $V^{(n)}$ approximate potential includes at most couplings between n different coordinates, and can be expressed as a linear combination of m-mode cuts ($m \leq n$) of the BO potential energy surface (PES), the particular linear combination avoids possible overcounting.[21] A generic n-mode cut is defined to be a section of the fully coupled PES, for which only n normal coordinates are different from zero and is denoted by $V^{\mathbf{m}_n}$, where $\mathbf{m}_n$ is a vector of n indices $m_1, m_2, \ldots, m_n$ (called a mode combination, MC, hereafter) for the n coordinates of the cut. The overcounting in the sum over $V^{\mathbf{m}_n}$ is avoided by defining a set of "intrinsic" potential terms,[21] $\bar{V}^{\mathbf{m}_n}$, such that they give zero if any of the n normal coordinates are zero (we follow the notation and general treatment of ref 21 hereafter):

$$\bar{V}^{\mathbf{m}_n}(\ldots, q_i = 0 \ldots) = 0 \tag{2}$$

The $\bar{V}^{\mathbf{m}_n}$ potentials are related to the $V^{\mathbf{m}_n}$ ones through[21]

$$\bar{V}^{\mathbf{m}_n} = S^{\mathbf{m}_n} \sum_{n'=1}^{n} (-1)^{n-n'} \binom{n}{n'} V^{\mathbf{m}_{n'}} \tag{3}$$

where $S^{\mathbf{m}_n}$ is an operator that symmetrizes with respect to the n m indices. The approximate adiabatic potential which includes up to n mode couplings is given in terms of the $\bar{V}^{\mathbf{m}_n}$[21]

$$V^{(n)} = \sum_{\mathbf{m}_k \in \mathrm{MCR}\{V\}} \bar{V}^{\mathbf{m}_k} \tag{4}$$

where MCR is the mode-combination range, or, in other words, the full set of MCs, up to a maximum number of mode couplings, n. Note that the procedure outlined above is general and every molecular property, in addition to the BO potential, is amenable to a similar hierarchical representation.

In this work, potential energy and property surfaces including couplings between at most n different modes have been generated via two different approaches. In the first approach, each $\bar{V}^{\mathbf{m}_k}$ potential term of eq 4 is represented as an m-order Taylor expansion, with expansion coefficients obtained by numerical differentiation around the equilibrium geometry.[21] In this work, all property surfaces, with the exception of the potential energy, are represented in this way, and will be denoted as *nMmT*. The order of the Taylor expansion is limited to 4 in this study. The Taylor expansion is done in normal coordinates and the step sizes employed in the numerical differentiation are chosen as described in ref 21.

Potential energy and molecular property surfaces can also be generated via a grid-based approach where the $\binom{M}{n}$ n-mode cuts of the BO PES, $V^{\mathbf{m}_n}$, are evaluated in a set of grid points by means of *ab initio* electronic structure calculations.[22] From the $V^{\mathbf{m}_n}$ values on the grids, the intrinsic terms of eq 2 are generated through eq 3 and are then spline-interpolated in a denser grid of points. A linear least-squares fit of the interpolated surfaces on a direct product polynomial basis[22] provides an analytical representation of the potential. In this work, all PESs are generated with a grid-based approach. The portions of the n-mode cuts of the PES to be sampled are selected through input of a non-negative integer υ in such a manner that the cutoff in the i-th normal coordinate axis for $V^{\mathbf{m}_n}$ corresponds to the classical turning point, $x_{i,\mathrm{TP}}$, for the harmonic motion in that direction:

$$x_{i,\mathrm{TP}} = \pm \sqrt{\frac{2\hbar}{\omega_i}\left(\upsilon + \frac{1}{2}\right)} \tag{5}$$

and multiplied by a scaling factor (in this study a factor of 1.2 has been used). In eq 5, ω_i is the harmonic frequency for the ith mode, and $\upsilon = 12$ has been used in this work. The mesh of evaluation points is linear and the interval length step is specified by giving the number of evaluation points. Flexibility is further enhanced by allowing the same number of evaluation points to be distributed more or less densely close to the reference (equilibrium) point. This is done by specifying a "fractioning" in the following manner: for a one-dimensional grid consisting of 64 evaluation points but with a fractioning of 1/2 the electronic structure calculations are carried out only in correspondence to the inner $64 \times 1/2 = 32$ displaced geometries around the reference structure, while a grid consisting of 32 evaluation points with no fractioning applied would result in a much more coarse grid covering the whole interval specified on input. This flexibility can conveniently be exploited when just the low-lying vibrational states are of interest since the portion of the PES sampled is reduced and therefore the total number of *ab initio* calculations.

A grid-based PES including up to three mode couplings will be denoted as $K_k L_l M_m$ with K, L, and M integers and the corresponding "fractionings" as subscripts.[22] With this notation, one-dimensional grids consist of $K*k$ uniformly spaced evaluation grid points, K being the maximum number up to the grid cutoff and k being the fraction of the grid. Two- and three-dimensional grids consist of $L*l$ and $M*m$ evaluation points,

respectively, for each of the normal coordinate axes. As an example, a $32_116_{3/4}$ PES is generated by including all one- and two-mode couplings, with each one-dimensional cut of the PES being sampled in a grid consisting of 32 evaluation points, whereas the two-dimensional cuts are sampled in grids consisting of $(16*3/4)^2 = 144$ evaluation points.

The total number of evaluation grid points can be calculated using

$$N_{\text{tot}} = \sum_{n=0}^{n_{\max}} \binom{M}{n} K_k^n \tag{6}$$

where $n_{\max}$ is the maximum number of modes coupled, M is the total number of modes, K_k^n is the number of grid points in the nth dimension, and $\binom{M}{n}$ is the binomial coefficient. For a system with 6 modes, this will give a total of 2353 grid points for a $32_116_{3/4}$ grid.

Either a low-order Taylor expansion or the linear least-squares fit provides a representation of the actual potential energy and molecular property operators in the computationally convenient sum-over-products form,[22]

$$O = \sum_{t=1}^{T} c_t \prod_{m=1}^{M} o^{m,t} \tag{7}$$

where $o^{m,t}$ may be any one-mode operator acting on a single mode, e.g., q, q^2, $\partial/\partial q$, and so forth.

In this work, all PESs are generated using the grid approximation employing, unless stated otherwise, a $32_{3/4}16_{3/4}8_{3/4}$ set of coarse grid points. Similarly, all molecular property surfaces are represented as fourth-order Taylor expansions including either 2, 3, or 4 mode combinations for the polyatomic species studied, providing *XM4T*, $X = 2$, 3, 4 surfaces.

B. Vibrational Averaging. The MidasCPP[23] program implements, among others, the VSCF [24−26] and VCI [25−30] methods for obtaining multimode wave functions and corresponding energies. For details on the VSCF and VCI methods, we refer to the above-mentioned references along with a recent review on vibrational wave functions.[31] Here, we present only the working equations used in the calculation of zero-point vibrational contributions in the VSCF and VCI approaches.

The ZPVC to a given property P is calculated according to

$$\langle P \rangle^{\text{ZPVC}} = \langle \Phi^K | P | \Phi^K \rangle \tag{8}$$

where K may refer either to a VSCF or a VCI wave function. If P includes the electronic contribution at the equilibrium geometry eq 8 defines the zero-point vibrational average (ZPVA) of the property. As noted above, the property operators are expressed as sum over products allowing for computationally very attractive formulations of algorithms for obtaining vibrational energies, wave functions, and so forth. For an operator $P = \sum_{t=1}^{T} c_t \prod_{m=1}^{M} p^{m,t}$, and the VSCF wave function (being a single Hartree product), this yields

$$\langle \Phi^{\text{VSCF}} | P | \Phi^{\text{VSCF}} \rangle = \sum_{t=1}^{T} c_t \prod_{m=1}^{M} \langle \varphi_{im}^m(q_m) | P^{m,t} | \varphi_{im}^m(q_m) \rangle \tag{9}$$

This is quite similar to evaluating the VSCF energy; see, e.g., ref 21. For a VCI wave function, the corresponding ZPVC becomes

$$\langle \Phi^{\text{VCI}} | P | \Phi^{\text{VCI}} \rangle = \sum_{r=1}^{R} \sum_{s=1}^{R} C_s \langle \Phi_s | P | \Phi_r \rangle C_r = \sum_{s=1}^{R} C_s \rho_s^p \tag{10}$$

where $\rho_s^p = \sum_{r=0}^{R} \langle \Phi_s | P | \Phi_r \rangle C_r$. Here, Φ_s and Φ_r are Hartree products and r and s correspond to two different occupation vectors. The calculation of the ZPVC is done via a transformer which provide the ρ_s^p intermediates of eq 10 and subsequently contract these with the relevant coefficients to yield the result. These steps are easy to implement based on the existing direct VCI framework for calculating the vibrational states themselves.

C. Thermal Effects. Focusing on the temperature dependence of the vibrational contributions to molecular properties, the canonical vibrational partition function can be written as[32]

$$Z^{\text{vib},T} = \sum_{i=0}^{\infty} \exp\left\{-\frac{\epsilon_i}{k_B T}\right\} \tag{11}$$

where we have neglected contributions due to the rotational−vibrational interaction, i.e., we assume a rigid-rotor approximation. In eq 11, the individual energies, ϵ_i, are calculated explicitly for all states. If the anharmonicity is small, the M mode partition function can be written as a direct product of partition functions for each of the modes with the anharmonic frequencies replacing the harmonic ones in the standard harmonic oscillator expressions. This method has been shown to provide good results for partition functions and thermodynamic properties.[33] In the present work, we will *not* assume such a separability and obtain the vibrational energies and states from vibrational calculations where the anharmonicity is included explicitly. Eq 11 has previously been used in a VSCF and VCI framework to calculate vibrational partition functions.[19,34]

Temperature averaged properties can be calculated by evaluating the expectation value of the property for each of the vibrational states included in the sum in eq 11, multiplied by the appropriate Boltzmann factor

$$\langle P \rangle^T = \frac{1}{Z^{\text{vib},T}} \sum_{i=0}^{\infty} P_i \exp\left\{-\frac{\epsilon_i}{k_B T}\right\} = \sum_{i=0} P_i W_i \tag{12}$$

where T is the temperature, P_i is the expectation value of the property in the ith vibrational state, and W_i the individual populations, normalized to one

$$W_i = \frac{1}{Z^{\text{vib},T}} \exp\left\{-\frac{\epsilon_i}{k_B T}\right\} \tag{13}$$

In order to calculate the thermal average, the property needs to be evaluated for all states, which of course becomes a formidable task for larger systems. Therefore, truncations in the number of states to be included in eq 12 must be employed. One way is to limit the summation to the subset having HO energies below a certain threshold. This is physically well motivated since the population of highly excited states is small at moderate temperatures, i.e., around 300 K. Using this simple scheme for truncating the state space, we can preselect the states to be calculated before doing any VSCF calculations.

A method based on the use of eqs 11 and 12 within a VSCF framework, with a (possibly large) number of states calculated state-specifically, will be denoted ss-VSCF. This means that in order to include N states, N VSCF calculations and vibrational averages must be performed.

An alternative approach within the VSCF framework is to calculate only the vibrational ground state. From such a calculation, one also obtains a set of eigenenergies for the virtual modals. One may now associate the energy differences from the vibrational ground state to another occupation with vibrational excitation energies. As the virtual states obtained in this fashion form an orthonormal set and have energies that separate into a sum of energies for the individual modes, the partition function for an M-mode system can be written as a simple product

$$Z = \prod_{m}^{M} z^{m} \tag{14}$$

We will refer to this method as v-VSCF. Thermal averages and thermodynamic properties may also be derived and calculated in a very efficient fashion. This v-VSCF method for efficiently obtaining partition functions and thermal averages is detailed in another paper.[35]

III. Computational Details

Geometry optimizations were performed using the DFT B3LYP functional [36,37] and, if not stated otherwise, the HuzIV-su4 basis set (details on this particular basis set is provided in the next section) followed by a normal-mode analysis supplying the harmonic frequencies and mass weighted normal coordinates in terms of Cartesian displacements. The normal-mode analyses have been performed for the relevant isotopomers in all molecules, since the normal coordinates and hence the PES and property surfaces expressed in normal coordinates will be changed. For acetylene, the H(1)C(13)C(13)H(1) isotopomer should be used when calculating the $^1J_{CC}$ SSCC, while the H(1)C(13)C(12)H(1) isotopomer should be used for the $^1J_{CH}$ and $^2J_{CH}$ SSCCs, and finally, the most common isotopomer H(1)C(12)C(12)H(1) should be used for the $^3J_{HH}$ SSCC. In principle, the C−H and H−H SSCCs should be averaged over all isotopomers according to their abundances, but this has not been done in the following analysis. The last isotopomer stated above will be the most abundant one, but due to the spin-free carbon-12 nuclei, no CC or CH SSCCs is observed experimentally.

The MidasCpp[23] program was used to generate the potential energy and property surfaces via an interface to the Dalton program package[38] which performed the needed single point electronic structure calculations. All property surfaces were Taylor expanded by including up to four mode couplings (for those molecules where possible) while the potential energy values computed on a set of grid points have been fitted to a direct product polynomial basis with a maximum degree of 12, thus improving the description of the potential further from the equilibrium geometry than the corresponding Taylor expanded surfaces. Note that quartic force field representations of molecular properties other than the energy are typically sufficient for accurate evaluations of ZPVCs.[22] The MidasCpp program was then used to perform the VSCF and VCI calculations of ZPVCs using the generated surfaces.

The primitive basis used for the vibrational calculations consist of one-mode harmonic oscillators (HO) with exponents fixed by the harmonic part of the potential. We have considered the effect of the size of the one-mode basis set in previous works, and found that seven HO basis functions are adequate for obtaining converged results for vibrational averages of other properties on similar molecules.[21]

We have confirmed that for the SSCCs calculated in the present work also we obtain sufficiently converged results at this one-mode basis set level (in all cases at least three significant digits).

In the following, the standard notation for spin−spin coupling constants has been adopted, i.e., $^2J_{CH}$ denotes a coupling between a carbon and a hydrogen atom separated by 2 bonds.

IV. Results and Discussion

A. Basis Set Investigation. Generating the potential and property surfaces based on numerical derivatives[21] or on a polynomial fit to a set of grid points (hereafter referred to as a grid method)[22] generally requires a great number of single point electronic structure calculations depending on the system size. The need to select a computationally cheap basis set still providing good quality is thus of great importance. Recently, Jensen[39] published a set of generally contracted basis sets which are shown to systematically converge the SSCCs to the density functional theory (DFT) basis set limit. These basis sets are based on the pc-*n* basis sets,[40] but augmented with tight s, p, d, and f functions as described in ref 39. Jensens basis sets are called pcJ-*n* and aug-pcJ-*n* depending on the inclusion of diffuse functions (aug) and the cardinal number minus one (*n*) meaning that the pcJ-1 is of double-ζ quality. In the present study, the performance of pcJ-*n* and aug-pcJ-*n* basis for $n = 0-4$ has been investigated and results obtained with the largest basis set have been used as reference when comparing to results obtained by employing other basis sets (see Supporting Information).

The popular Huzinaga[41] basis sets have successfully been used for uncorrelated calculations of SSCCs.[12,42−44] They must, however, be augmented by polarization functions, as by Kutzelnigg et al.,[45] and in addition, the s functions should be decontracted. Furthermore also a number of tight s functions should be added thereby defining the Huz*N*-sun basis sets where $N = $ I, II, III, IV and $n = 1, 2, 3, 4$. These basis sets were used by Ruden et al. in ref 12 and have been tested as well.

The basis set analysis revealed that the HuzIV-su4 basis set generally produces results in very good agreement with the (aug-)-pcJ-4 results to within a few percent (with the exception of the N_2 molecule), despite this basis set being roughly the size of the pcJ-2 one. The HuzIV-su4 basis set therefore provides a good compromise between computational cost and accuracy and we will use this basis set for the large number of grid point calculations. Results of the basis set investigation in tabular form are included as Supporting Information.

SSCCs are quite dependent on the molecular structure and hence inaccuracies in the calculated optimized geometries will be reflected in the SSCCs and their zero-point averages. However, a study of the equilibrium geometries and harmonic frequencies calculated by the Huz-IVsu4 basis set and the standard aug-cc-pVTZ basis showed that the differences are negligible, with deviations in equilibrium geometries being at most a few tenths of a picometer, angles less than one-tenth of a degree, and harmonic frequencies less than 5 cm^{-1}.

B. Investigation of Mode-Coupling Level in Property Surfaces. As briefly outlined above, the potential energy surfaces and property surfaces are calculated via two different methods: either as a low-order Taylor expansion in the normal modes or by fitting data points computed on a grid using a linear least-squares fitting in a direct-product polynomial basis. The latter is the most robust and accurate approach, since it allows for an accurate description of the potential much further away from the equilibrium geometry. It is, however, also the most expensive in terms of the number of single point electronic structure calculations which need to be performed.

In this work, property surfaces are represented by fourth-order Taylor expansions, whereas the PESs are calculated via the grid approach. In the following, we will investigate the effect of the mode-coupling level in the property surfaces.

For the three diatomics (HF, CO, and N_2) studied here, there is only one mode, and hence studying the mode-coupling level for these is meaningless. Results for the polyatomics are presented in Tables 1, 2, 3, and 4 for water (H_2O), hydrogen cyanide (HCN), acetylene (C_2H_2), and methane (CH_4), respectively.

The mode-coupling level in the property surfaces has a very limited effect on the computed SSCCs for the water molecule (Table 1), the largest difference being less than 0.1% ($^2J_{HH}$

TABLE 1: Zero-Point Vibrational Contributions to the Isotropic $^1J_{OH}$ and $^2J_{HH}$ Spin−Spin Coupling Constants for H_2O at the VSCF/VCI Levels Using Harmonic Oscillator Basis Sets[a]

	VSCF	VCI[2]	VCI[3]
$^1J_{OH}$			
2M4T	5.392	5.336	5.332
3M4T	5.392	5.336	5.332
$^2J_{HH}$			
2M4T	0.8247	0.8383	0.8402
3M4T	0.8247	0.8388	0.8405

[a] Values are in Hz. The given mode combinations (XM4T, X = 2, 3) are used for all property surfaces while a $32_{3/4}16_{3/4}8_{3/4}$ set of coarse grid points has been used in constructing the PES.

TABLE 2: Zero-Point Vibrational Contributions to the Isotropic Spin−Spin Coupling Constants for HCN Calculated at the VSCF/VCI Levels Using Harmonic Oscillator Basis Sets[a]

	VSCF	VCI[2]	VCI[3]	VCI[4]
$^1J_{HC}$				
2M4T	5.465	5.416	5.385	5.385
4M4T	5.464	5.416	5.386	5.387
$^1J_{CN}$				
2M4T	1.804	1.847	1.831	1.831
4M4T	1.804	1.847	1.831	1.831
$^2J_{HN}$				
2M4T	0.8203	0.8492	0.8417	0.8417
4M4T	0.8202	0.8491	0.8421	0.8422

[a] Values are in Hz. The given mode combinations (XM4T, X = 2, 3, 4) are used for all property surfaces while a $32_{3/4}16_{3/4}8_{3/4}$ set of coarse grid points has been used in constructing the PES.

TABLE 3: Zero-Point Vibrational Contributions to the Isotropic Spin−Spin Coupling Constants $^1J_{CC}$, $^1J_{CH}$, $^2J_{CH}$, and $^3J_{HH}$ for C_2H_2 at the VSCF/VCI Levels Using Harmonic Oscillator Basis Sets[a]

	VSCF	VCI[2]	VCI[3]	VCI[4]
$^1J_{CC}$				
2M4T	−7.950	−8.302	−8.607	−8.644
3M4T	−7.950	−8.302	−8.629	−8.667
4M4T	−7.950	−8.302	−8.630	−8.669
$^1J_{CH}$				
2M4T	5.296	5.232	5.202	5.197
3M4T	5.295	5.233	5.159	5.151
4M4T	5.295	5.233	5.161	5.156
$^2J_{CH}$				
2M4T	−2.444	−2.645	−2.759	−2.776
3M4T	−2.444	−2.644	−2.847	−2.869
4M4T	−2.444	−2.644	−2.847	−2.869
$^3J_{HH}$				
2M4T	0.0373	−0.0110	−0.0374	−0.0406
3M4T	0.0372	−0.0111	−0.0576	−0.0619
4M4T	0.0372	−0.0111	−0.0581	−0.0622

[a] Values are in Hz. The given mode combinations (XM4T, X = 2, 3, 4) are enforced on all property surfaces while a $32_{3/4}16_{3/4}8_{3/4}$ set of coarse grid points has been used in constructing the PES.

calculated at the VCI[2] level). The mode-excitation level of the vibrational wave function is of greater importance judging from the difference between VSCF and VCI[2]. Already at the VCI[2] level the results are converged to the VCI[3] (FVCI) results within a few thousandths of a Hz.

The results for the HCN molecule are presented in Table 2. The convergence with respect to the mode-coupling level in the property surfaces resembles that for the water molecule. The 3M4T results are not included since there is only one 4-mode coupling term and the difference between P3M4T and P4M4T results is negligible. A mode-excitation level of three in the VCI calculation gives results that are converged to the FVCI results within 0.001 Hz, while VCI[2] has differences of up to 0.04 Hz.

TABLE 4: Zero-Point Vibrational Contributions to the Isotropic Spin−Spin Coupling Constants for CH_4 at the VSCF/VCI Levels Using Harmonic Oscillator Basis Sets[a]

	VSCF	VCI[2]	VCI[3]	VCI[4]
$^1J_{CH}$				
2M4T	5.711	5.742	5.755	5.758
3M4T	5.711	5.743	5.753	5.756
4M4T	5.711	5.743	5.753	5.756
$^2J_{HH}$				
2M4T	−0.7040	−0.7190	−0.7228	−0.7233
3M4T	−0.6944	−0.7022	−0.7086	−0.7092
4M4T	−0.6944	−0.7022	−0.7061	−0.7051

[a] Values are in Hz. The given mode combinations (XM4T, X = 2, 3, 4) are used for all property surfaces while a $32_{3/4}16_{3/4}8_{3/4}$ set of coarse grid points have been used in constructing the PES.

The mode-coupling level in the property surfaces does not appreciably affect the VSCF and VCI[2] results for C_2H_2, reported in Table 3. Convergent results are, however, obtained only by allowing an excitation level of 3 or 4 in the VCI wave function and with the inclusion of three-mode couplings in the computed property surfaces. Inclusion of 4-mode terms in the representation of the property surfaces seems to have very little effect (less than 0.001 Hz) on the VCI[3] and VCI[4] results. Although the VCI[2] model represents a good improvement over the VSCF approximation, VCI[2] gives results which are still off from the VCI[4] ones by up to several tenths of a Hz. The differences between VCI[2] and VCI[3] are about as large as those between VSCF and VCI[2]. For higher excitation levels, the corrections are smaller by roughly 1 order of magnitude.

The results for the methane molecule are shown in Table 4. The convergence of the results with respect to the mode-combination level used in the representation of the property surfaces is roughly the same as that found for the acetylene molecule, although 4-mode coupling terms are of greater importance for the $^2J_{HH}$ results. The contributions from the 4-mode terms are still somewhat smaller than those for the 3-mode contributions. With respect to the mode-excitation level in the VCI wave function, the results are close to convergence already at the VCI[2] level, with deviations from VCI[4] of less than 1%. This is in contrast to what was found for the acetylene molecule.

In conclusion, we find that for the polyatomic molecules studied here, the mode-excitation level in the wave function is generally of greater importance than the mode combination level used in the property surfaces beyond two-mode combinations. Restricting ourselves to two-mode couplings for the property surface leads in the present case to errors of a few hundredths of a Hz or less.

We note here that using VCI[2] in combination with 2M4T property surfaces generally provides a good description of ZPVCs to SSCCs (with the exception of acetylene where VCI[3] is needed).

C. Variational Approaches Vs Perturbation Theory. To second order in perturbation theory (where the uncoupled harmonic oscillator is the zeroth-order description) one may

express the zero-point vibrational contributions to a molecular property as, e.g., refs 12, 46

$$\langle P\rangle^{\mathrm{ZPVC}} = \frac{1}{4}\sum_{K=1}^{M}\frac{\mathrm{d}^2P}{\mathrm{d}Q_K^2}\frac{1}{\omega_K} - \frac{1}{4}\sum_{K=1}^{M}\frac{\mathrm{d}P}{\mathrm{d}Q_K}\frac{1}{\omega_K^2}\sum_{L=1}^{M}\frac{\mathrm{d}^3V}{\mathrm{d}Q_K\mathrm{d}Q_L^2} \quad (15)$$

In MidasCpp the operators are represented as sum-over-products (SOP) operators. Therefore, the derivatives needed to evaluate eq 15 are readily available, as they are related to the expansion coefficients of the SOP terms by a simple factor and the VPT expression (eq 15) has been implemented as a simple byproduct.

In Table 5 we present vibrational contributions calculated by VCI[2] using different vibrational basis sets and operators. The results are deviations from the "best" results calculated using the best surfaces and vibrational structure methods. One thing to notice is the great flexibility when using vibrational structure theory, i.e., VSCF, VCI, and so forth, compared to the standard perturbation theory formalism. In the former approach one has the possibility of adjusting the excitation level used at the wave function level, the size of the vibrational basis set, and the representation of the operators. As a consequence one has the possibility of mirroring closely the perturbation theory results by simply performing a VCI[2]/$v = 1$ calculation, employing V2M3T/P1M2T surfaces. However, due to the variational procedure this is usually a bad choice, as this potential is unbound, and, in particular, the one mode part was found to be a problem. Hence, we explore the addition of the 1M4T terms as well. It should be noted that this does not increase the computational complexity of the surfaces based on calculations of energy points, as the fourth-order terms may be calculated from the same points as the third-order terms.

For the molecules presented in Table 5 it is clear that both VPT and many of the variational combinations perform rather well compared to the reference results when judged by the mean absolute deviation. VCI[2] calculations using a mode combination level of two in the surfaces, i.e., also in the PES, which included 3 MCs in the previous section, seem to provide a well-balanced description of the ZPVCs, providing the best results with respect to the reference values based on both the mean and maximum absolute deviations. This is important since vibrational computations based on an excitation level of two and using two-mode operators may be performed in a very efficient manner,[47] and the computational cost of the vibrational calculations at this level is vanishing relative to the cost of generating the energy and property surfaces.

It is also evident that VCI[2] with V2M3T+1M4T/P1M2T surfaces using a $v = 1$ basis set is, with the exception of the H_2O $^1J_{OH}$ and CH_4 $^1J_{CH}$ SSCCs, very close to the perturbation theory values. The differences are due to the small rotations of the modals which are still possible in the variational procedure even for this very simple calculation. Using the same operators and increasing the vibrational basis set does not generally provide results that are better than the perturbation theory results.

The last column in Table 5 represent the simplest potential and property surfaces which include the effect of anharmonicity in the PES, i.e., V1M4T/P1M2T surfaces are used resulting in the uncoupled anharmonic oscillator (UAO) result. Clearly the UAO approximation is too severe to provide accurate results. This observation is not surprising, as anharmonic mode coupling is necessary for accuracy.

In conclusion, we note that VPT performs fairly well for these stiff molecules. Furthermore, the variational procedure may provide results with similar accuracy as the VPT using roughly the same overall computational effort. Moreover, it is possible to increase the accuracy of the variational approach in rigorous manner by varying (i) the variational basis set used to expand the individual modes, (ii) the description of the surfaces used,

TABLE 5: Comparison of SSCCs for the Polyatomic Molecules Calculated by Different VCI Methods and Vibrational Operators/Basis Sets as Well as Using the Perturbation Theory Approximation[a]

		VCI[2]								VPT[b]	UAO[c]
SSCC	PES property reference[h]	grid[d] Taylor[d]	$32_{3/4}16_{3/4}$ 2M4T	2M4T 1M4T	2M4T 1M2T	2M4T 1M2T	2M3T[e] 1M2T	2M3T[f] 1M2T	2M3T[g] 1M2T		1M4T 1M2T
					H_2O						
$^1J_{OH}$	5.333	−0.006	−0.205	−0.066	−0.052	−0.021	0.348	−0.133	−0.381	0.034	3.374
$^2J_{HH}$	0.8405	0.002	0.041	0.024	−0.057	−0.045	−0.038	0.038	0.067	−0.048	−0.738
					HCN						
$^1J_{CH}$	5.387	−0.029	0.082	0.170	0.597	0.762	0.179	0.268	0.284	0.192	−2.473
$^1J_{CN}$	1.831	−0.016	−0.092	−0.100	−0.117	−0.249	−0.106	−0.045	−0.049	−0.110	−0.258
$^2J_{NH}$	0.8422	−0.007	−0.031	−0.034	0.077	−0.005	0.009	0.031	0.031	0.009	−0.202
					CH_4						
$^1J_{CH}$	5.756	0.014	−0.070	0.093	0.136	0.186	0.531	0.342	0.264	0.381	2.897
$^2J_{HH}$	−0.7051	0.014	−0.037	−0.027	−0.143	−0.148	−0.038	−0.058	−0.060	−0.042	0.158
					C_2H_2						
$^1J_{CC}$	−8.669	−0.367	0.149	−0.045	−0.106	0.499	0.509	0.091	0.091	0.517	−1.464
$^1J_{CH}$	5.156	−0.076	0.084	0.163	0.227	0.207	0.285	0.167	0.161	0.296	−1.684
$^2J_{CH}$	−2.869	−0.224	0.012	−0.055	−0.274	−0.065	0.038	−0.151	−0.152	0.044	−0.731
$^3J_{HH}$	−0.062	−0.051	−0.033	−0.034	−0.120	−0.069	−0.004	−0.046	−0.049	−0.004	−0.001
MAD[I]		0.073	0.076	0.074	0.173	0.205	0.190	0.125	0.144	0.152	1.271
MAXAD[I]		0.367	0.205	0.170	0.597	0.762	0.531	0.342	0.381	0.517	3.374

[a] Values are provided in Hz relative to the reference value and in all cases represent the best variational calculation. If not stated otherwise the calculations use a $v = 6$ basis for all modes. [b] VPT (vibrational perturbation theory). [c] UAO (uncoupled anharmonic oscillators). [d] Using the same surfaces as the reference. [e] Using a $v = 1$ vibrational basis set. The PES also contains 1M4T terms. [f] Using a $v = 2$ vibrational basis set. The PES also contains 1M4T terms. [g] Using a $v = 6$ vibrational basis set. The PES also contains 1M4T terms. [h] This work calculated using the best VCI wave functions and best surfaces. [I] MAD (mean absolute deviation), MAXAD (maximum absolute deviation).

TABLE 6: Calculated SSCCs Compared to Experimental Values[a]

SSCC	B3LYP[b]	B3LYP[c]	CCSD[d]	SOPPA[e]	CC3[d]	Vib[b]	J_{Emp}	J_{Exp}
				HF				
$^1J_{HF}$	424.9	416.6	521.6	529.4	521.5	−37.81	537.8	500[f]
				CO				
$^1J_{CO}$	17.7	18.4	15.7	18.6	15.3	0.694	15.7	16.4[f]
				N_2				
$^1J_{NN}$	1.17	1.4	1.8	2.1	1.77	0.102	1.7	1.8[f]
				H_2O				
$^1J_{OH}$	−76.9	−75.9	−78.9	−80.6	−78.52	5.33	−85.93	−80.6[g]
$^2J_{HH}$	−7.21	−7.5	−7.8	−8.8	−7.35	0.841	−8.04	−7.2[h]
				HCN				
$^1J_{CH}$	284.7	283.5	245.8		242.1	5.39	261.9	267.3[j]
$^1J_{CN}$	−19.8	−19.2	−18.2		−17.90	1.83	−20.33	−18.5[j]
$^2J_{HN}$	−8.04	−7.8	−7.7		−7.65	0.842	−9.54	−8.7[j]
				CH_4				
$^1J_{CH}$	133.8	132.6		122.3		5.76	119.5	125.3[j]
$^2J_{HH}$	−13.5	−13.3		−14.0		−0.705	−12.1	−12.8[j]
				C_2H_2				
$^1J_{CC}$	206.2	205.1		190.0		−8.67	183.5	174.8[j]
$^1J_{CH}$	273.4	271.9		254.9		5.16	242.4	247.6[j]
$^2J_{CH}$	56.7	56.0		51.7		−2.87	53.0	50.1[j]
$^3J_{HH}$	11.0	10.6		11.3		−0.062	9.66	9.6[j]

[a] The experimental values have been corrected with the calculated vibrational contributions to give the $^kJ_{XY}^{emp}$ values used for comparison. Values are in Hz. [b] This work calculated using the best VCI wave functions and best surfaces. [c] ref 12. [d] ref 53 [e] HF, CO, N_2, H_2O, and CH_4 are from ref 54. The C_2H_2 results are from ref 55. [f] HF, CO, and N_2 are adapted from refs 56, 57, and 58, respectively. [g] ref 59. [h] ref 60. [j] HCN, CH_4, and C_2H_2 are from refs 61, 62, and 63 respectively.

and (iii) the level of mode−mode correlation included in the vibrational wave function.

D. Comparison with Experiment. In the following we will compare our results with the available experimental data. Although DFT has proven somewhat successful in calculating SSCCs at the equilibrium geometry, the comparison of DFT based results to experimental data can sometimes be problematic. This is most pronounced for nuclei having lone pairs and especially in the case of fluorine containing compounds, for which many DFT functionals are known to provide SSCCs of poor quality [48−52] even when vibrational contributions are added.[12] One might hope, however, that the error introduced by DFT will be roughly constant when the SSCCs are evaluated at different geometries and hence provide property surfaces which pertain only a minimum of the error. Therefore, vibrational contributions calculated at the DFT level may be of reasonable quality even though the value at the equilibrium geometry is not and must therefore be calculated at a higher level of accuracy.

Table 6 reports SSCCs calculated at the equilibrium geometry for the set of molecules considered in this work as well as CC3 results taken from the literature. In the following we have chosen to subtract our vibrational contribution from the experimental results rather than correcting the equilibrium values. This defines a new empirical SSCC

$$J^{emp} = J^{exp} - J^{vib} \tag{16}$$

For the DFT results one notice that there are slight discrepancies between the equilibrium results calculated in this work and the results from ref 12. This is due to the different construction of the B3LYP functional; the results of ref 12 are obtained with the VWNI functional while the VWN5 functional for local correlation is used in the present work. In ref 12 vibrational corrections were also calculated using perturbation theory.

Since these molecules are relatively rigid and good candidates for perturbation theory as confirmed in the previous subsection, our results confirm overall the perturbational results of ref 12. The results are numerically rather similar and their difference is minor relative to the discrepancy between theory and experiment as we shall discuss below.

1. Diatomics. For the diatomic molecules considered in the present work, the DFT equilibrium SSCCs are of varied quality with respect to the empirical SSCCs. For the CO molecule the equilibrium SSCC is actually closer to the experimental result than the empirical one. The CC3 results are generally in good agreement with the calculated empirical results and clearly the inclusion of ZPVCs bring the CC3 SSCCs into closer agreement with the experimental values.

2. Polyatomics. In contrast to what was observed for the diatomics, inclusion of ZPVCs generally does not improve the agreement between the CC3 results and the experimental values for water and hydrogen cyanide. For these two molecules the trend is rather that the agreement becomes better when the SSCC is positive (only for the $^1J_{CH}$ SSCC), whereas it becomes worse when it is negative. In fact for all SSCCs except the $^2J_{HH}$ and $^2J_{HH}$ SSCCs for water, the pure DFT results are in closer agreement with the empirical value.

For methane and acetylene, comparison with CC3 results is hampered, since to the best of the authors' knowledge, the latter are not reported in the literature. The addition of ZPVCs to the DFT results generally does not provide a better agreement with experimental data. The agreement is worsened for methane, whereas the agreement for most of the acetylene SSCCs is only slightly improved.

E. Temperature Dependence of SSCCs. In the following we will investigate the temperature dependence of selected spin−spin coupling constants. Temperature effects for the molecules studied so far are expected to be rather limited due to the lack of low-frequency modes, e.g., the lowest mode of

TABLE 7: Thermal Contributions to SSCCs for All the Polyatomic Molecules Studied, Calculated with the ss-VSCF and v-VSCF Methods[a]

		ss-VSCF				v-VSCF			
SSCC	eq[b]	100 K	200 K	300 K	400 K	100 K	200 K	300 K	400 K
					H_2O				
$^1J_{OH}$	−76.94	5.387	5.387	5.386	5.375	5.387	5.387	5.386	5.380
$^2J_{HH}$	−7.21	0.825	0.826	0.828	0.841	0.825	0.826	0.828	0.840
					HCN				
$^1J_{CH}$	284.7	5.464	5.474	5.528	5.629	5.464	5.492	5.654	5.964
$^1J_{CN}$	−19.8	1.804	1.809	1.834	1.882	1.804	1.811	1.850	1.925
$^2J_{HN}$	−7.2	0.820	0.822	0.834	0.855	0.820	0.824	0.846	0.888
					CH_4				
$^1J_{CH}$	133.8	5.710	5.710	5.718	5.754	5.710	5.710	5.721	5.766
$^2J_{HH}$	−13.5	−0.691	−0.691	−0.693	−0.699	−0.691	−0.691	−0.693	−0.699
					C_2H_2				
$^1J_{CC}$	206.2	−7.950	−8.047	−8.470	−9.166	−7.950	−8.023	−8.358	−8.928
$^1J_{CH}$	273.4	5.358	5.276	5.209	5.116	5.296	5.312	5.420	5.641
$^2J_{CH}$	56.7	−2.444	−2.489	−2.683	−3.004	−2.444	−2.477	−2.625	−2.876
$^3J_{HH}$	11.0	0.037	0.027	−0.015	−0.086	0.037	0.030	−0.001	−0.052
					C_2H_4				
$^1J_{CC}$	76.2	1.083	1.083	1.086	1.094	1.083	1.085	1.104	1.156
					C_2F_4				
$^1J_{CC}$	218.3	−1.167	−1.296	−1.694	−2.247	−1.149	−1.184	−1.465	−1.918
					C_2Cl_4				
$^1J_{CC}$	137.0	0.2574	0.5490	0.8295	1.076	0.2553	0.5372	0.7968	1.027

[a] The surfaces are calculated with DFT using the B3LYP functional in the HuzIV-su4 (H_2O, HCN, CH_4, and C_2H_2) or aug-pcJ-1 basis (C_2H_4, C_2F_4, and C_2Cl_4). The vibrational calculations use a $v = 4$ basis. Values are in Hz. [b] All equilibrium values are calculated using the HuzIV-su4 basis except for ethene and its analogues as described in the text.

water is 1593 cm^{-1} to be compared with $k_BT \simeq 208$ cm^{-1} at room temperature. Therefore, in this section an additional set of molecules is analyzed, namely, ethene and some of its tetra-halogenated analogues, i.e., tetra-fluoroethene and tetra-chloroethene. Due to the presence of lower-frequency modes in the tetra-halogenated species one can expect a higher population of excited vibrational states. For the tetra-chloro analogue, a harmonic frequency of just 95 cm^{-1} is found based on a B3LYP/apcJ-1 calculation. For the chlorine containing compound, we have used the apcJ-2 basis set[39] to predict the equilibrium geometry values. The apcJ-2 basis set was found to provide results that are very close to the ones obtained with Huz-IVsu4 (the actual results are available as Supporting Information). For computational economy in the generation of the surfaces we have used the smaller apcJ-1 basis set.

The PESs are calculated from a $32_{3/4}16_{3/4}$ set of grid points giving a total of 9793 single point calculations. Extra grid points have been obtained by interpolation and fitted to a 12 degree polynomial. The property surfaces are 2M4T expansions around the equilibrium geometry.

One problem inherent in the calculation of thermal averages based on the expressions derived from statistical mechanics is that the sum in eq 11 extends in principle to all possible states. For the 12 mode systems studied here and by expanding each modal in a basis consisting of 5 HO functions already result in more than 10^9 states that need to be included, making this approach unpractical. However, at low/moderate temperatures the contributions from highly excited states will become negligible due to the exponentially decaying Boltzmann factor and thus many states can safely be neglected. In the following this method of truncation of the ss-VSCF state space has been used with varying energy thresholds in order to obtain converged results. For the v-VSCF method, on the other hand, the complete state space is trivially explored due to the formalism of the method. However, the v-VSCF description is greatly simplified and thus potentially less accurate.

The thermal contributions for all polyatomic species are presented in Table 7 along with the equilibrium values. Note that the equilibrium values should be added to the thermal contributions in order to obtain the thermally averaged SSCCs. By considering the ss-VSCF results for H_2O, HCN, CH_4, and C_2H_2, one sees that thermal effects are somewhat limited for the majority of the molecules, as expected due to the lack of low-frequency modes. The most pronounced effect is found for the acetylene $^1J_{CC}$ with the result at 400 K being 15% larger in magnitude than the 0 K one. However, the temperature effects at 300 K are already significant for some of these molecules compared to the effects of the details of the vibrational wave function level and surface model.

The v-VSCF results are in reasonable agreement with the ss-VSCF results with deviations of less than 10% with respect to the ss-VSCF results in all cases, with the exception of the $^3J_{HH}$ SSCC for acetylene and the $^1J_{CC}$ SSCC for tetra-fluoroethene. The results are quite satisfactory, taking into account the very simple ansatz for the model, i.e., doing a ground-state VSCF optimization and using the resulting energy differences between virtual and occupied modals as excitation energies, and basing the vibrational averages on the corresponding virtual wave functions. In another paper it has been demonstrated that the v-VSCF method for calculating thermal averages provides qualitatively correct results compared to the explicit sum-over-states expressions, provided that the vibrational basis set is large enough to describe the increasing population of higher-energy states with increasing temperature.[35] In case of an insufficient vibrational basis, neither of the methods can be expected to give good results. Consider, for example, a mode with a fundamental frequency of 200 cm^{-1}. Expressing this modal in, e.g., five basis functions will not capture the full

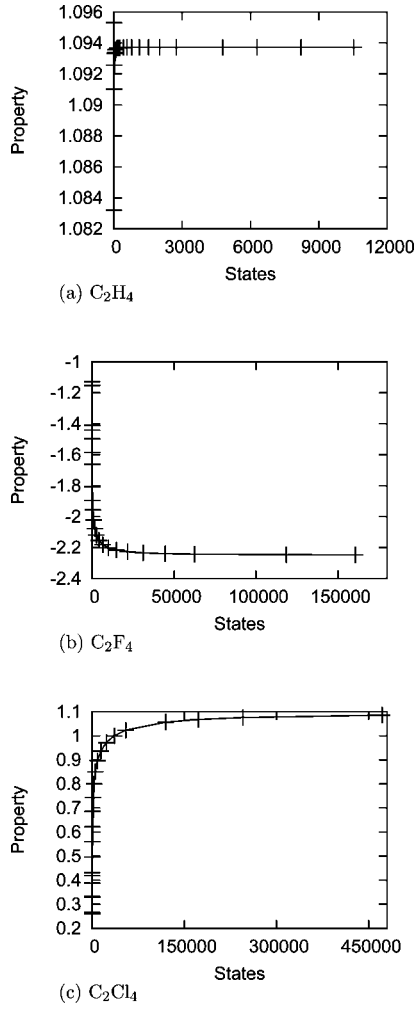

Figure 1. Convergence of the ss-VSCF thermal average of the $^1J_{CC}$ SSCC for the C_2X_4; X = H, F, Cl molecules as a function of the number of states. Values are in Hz.

thermal effect at higher temperatures due to neglect of the population of higher excited states in that mode.

In Figure 1 the convergence of the thermal averages of the $^1J_{CC}$ couplings with respect to the number of states included for ethene and the tetra-halogenated analogues is plotted for different truncations of the state space. For ethene the convergence is very fast with less than 1000 states needed to obtain $^1J_{CC}$ SSCC converged to within 10^{-5} even at 400 K. The v-VSCF and ss-VSCF results are generally in good agreement.

For the flourine analogue the convergence is slower due to the presence of lower-frequency modes. The inclusion of approximately 120 000 states provides a $^1J_{CC}$ SSCC thermal-averaged value which is converged to 10^{-3} Hz at 400 K. At 300 K, roughly room temperature, the convergence is, however, faster and about 50 000 states are needed in order to obtain convergence of the SSCC within 1 mHz with respect to the 245 000 states result. The v-VSCF results are not as close to the ss-VSCF results as for ethene.

Because of the very low frequency modes the convergence is even slower for the tetrachloro analogue. The 400 K results for the SSCC thermal average presented in Figure 1c do not seem to be fully converged even with the inclusion of as many as 470 000 states. The difference in the thermal averages of the SSCC obtained by including 245 000 and 470 000 states are on the order of 10^{-2} or about 1% of the total thermal average. The result at 300 K, however, converge faster although 170 000 states are still needed for converging the thermal average to within 1 mHz (with respect to the 470 000 states result). The v-VSCF results are in good agreement with the ss-VSCF results, also better than for tetra-fluoroethene.

From the figure it is evident that as one increases the temperature the excited vibrational states become more populated. For ethene the effect is quite small for all temperatures studied here and can be regarded as a direct consequence of the system lacking modes of low frequencies resulting in low populations of the excited states. The effect become more pronounced for the tetra-halogenated species. For the tetrachloroethene molecule the effect at room temperature is very important with a thermally averaged value of approximately 0.83 Hz corresponding to a ZPVC value of 0.1450 Hz. This large difference is due solely to the thermal contributions.

The results obtained with the v-VSCF and ss-VSCF methods at selected temperatures are compared in Table 7. The two sets of results are quite close for ethene and the chloro analogue, while they, as discussed above, differ somewhat more for C_2F_4.

V. Summary

In this paper we have calculated zero-point vibrational contributions to indirect spin−spin coupling constants for N_2, CO, HF, H_2O, C_2H_2, and CH_4 via explicit anharmonic approaches. In addition, we have presented thermal averages of indirect spin−spin coupling constants for C_2X_4, X = H, F, Cl. Potential energy surfaces have been calculated with a grid-based approach and analytic representations have been obtained with a linear least-squares fit in a direct product polynomial basis. The property surfaces have been calculated by using fourth-order Taylor expansions around the equilibrium geometry. The electronic structure calculations are performed using density functional theory and vibrational contributions to indirect spin−spin coupling constants are calculated by employing the vibrational self-consistent field and vibrational configuration interaction methods. For the calculations of the thermal averages we have used both state-specific and virtual vibrational self-consistent field methods. In general we find that for the polyatomic molecules the mode-excitation level in the wave function is of greater importance than the mode combination level included in the property surfaces, i.e., a two-mode combination included in the property surfaces leads in the present case to errors of a few hundredths of a Hz or less. For the set of diatomic molecules studied in this work, inclusion of vibrational effects leads to an enhanced agreement between theory and experimental data. For the polyatomic molecules, on the other hand, the picture is changed. Here, inclusion of vibrational effects does not lead to a consistent improvement of the results. In fact, for one molecule (methane) the agreement between theoretical and experimental data is worsened upon correcting for vibrational effects.

The good performance of vibrational perturbation theory calculations of SSCCs often assumed for fairly rigid molecules is confirmed in this study by comparison with more rigorous calculations. Furthermore, based on a detailed series of calculations we argue that one may use the VCI approach in connection with a simple representation of the surfaces to obtain results of similar accuracy with overall similar computational effort. For the variational methods, such as VCI, one has the possibility to extend the accuracy of the computed results in a rigorous manner which is believed to be a significant advantage. For example, VCI[2] with two-mode fourth-order Taylor potential and property surface appears to be another cost-efficient compromise.

Concerning the thermal averages of the SSCCs, a significant temperature dependence is found for molecules possessing low

vibrational frequencies. A reasonably good agreement between the two different methods of introducing temperature effects, i.e., the v-VSCF and ss-VSCF methods, is generally found. This is highly encouraging in view of the computational economy of the virtual vibrational self-consistent-field method in ref 35 as compared to the state-specific VSCF approach of refs 19, 34.

Acknowledgment. This work has been supported by the Lundbeck foundation and DCSC (Danish Center for Scientific Computing). J.K. acknowledges support from the Villum Kann Rasmussen Foundation. O.C. acknowledges support from the Danish national research foundation, the Lundbeck Foundation, and The Danish Natural Science Research Council (Grant No. 21-04-0268), and EUROHORCs through a EURYI award. We thank H. J. Aa. Jensen and F. Jensen for useful comments.

Supporting Information Available: The results obtained in the basis set study are provided in tabular form. This material is available free of charge via the Internet at http://pubs.acs.org.

References and Notes

(1) Helgaker, T.; Jaszuński, M.; Ruud, K. *Chem. Rev.* **1999**, *99*, 293.
(2) Autschbach, J.; Ziegler, T. *J. Chem. Phys.* **2000**, *103*, 936.
(3) Filatov, M.; Cremer, D. *J. Chem. Phys.* **2004**, *120*, 11407.
(4) Autschbach, J.; Ziegler, T. *Coord. Chem. Rev.* **2003**, *238*−*239*, 83.
(5) Autschbach, J. *Coord. Chem. Rev.* **2007**, *251*, 1796.
(6) Barfield, M.; Smith, W. B. *J. Am. Chem. Soc.* **1992**, *114*, 1574.
(7) Russell, A.; Spackman, M. *Mol. Phys.* **1996**, *88*, 1109.
(8) Wigglesworth, R. D.; Raynes, W. T.; Sauer, S. P. A.; Oddershede, J. *Mol. Phys.* **1998**, *95*, 851.
(9) Sauer, S. P. A.; Møller, C. K.; Koch, H.; Paidarová, I.; Spirko, V. *Chem. Phys.* **1998**, *238*, 385.
(10) Åstrand, P.-O.; Ruud, K.; Taylor, P. R. *J. Chem. Phys.* **2000**, *112*, 2655.
(11) Ruud, K.; Åstrand, P.-O.; Taylor, P. R. *J. Chem. Phys.* **2000**, *112*, 2668.
(12) Ruden, T. A.; Lutnæs, O. B.; Helgaker, T.; Ruud, K. *J. Chem. Phys.* **2003**, *118*, 9572.
(13) Mort, B.; Autschbach, J. *J. Am. Chem. Soc.* **2006**, *128*, 10060.
(14) Ramsey, N. *Phys. Rev.* **1953**, *91*, 303.
(15) Helgaker, T.; Jaszuński, M.; Ruud, K.; Górska, A. *Theor. Chem. Acc.* **1998**, *99*, 175.
(16) Peralta, J.; Scuseria, G.; Cheeseman, J.; Frisch, M. *Chem. Phys. Lett.* **2003**, *375*, 452.
(17) Fukui, H. *Prog. NMR Spectrosc.* **1999**, *35*, 267.
(18) Helgaker, T.; Watson, M.; Handy, N. C. *J. Chem. Phys.* **2000**, *113*.
(19) Kongsted, J.; Christiansen, O. *J. Chem. Phys.* **2007**, *127*, 154315.
(20) Hirata, S.; Yagi, K.; Perera, S. A.; Yamazaki, S.; Hirao, K. *J. Chem. Phys.* **2008**, *128*, 214305.
(21) Kongsted, J.; Christiansen, O. *J. Chem. Phys.* **2006**, *125*, 124108.
(22) Toffoli, D.; Kongsted, J.; Christiansen, O. *J. Chem. Phys.* **2007**, *127*, 204106.
(23) MidasCpp (Molecular Interactions, dynamics and simulation Chemistry program package in C++), http://www.chem.au.dk/~midas, 2008.
(24) Bowman, J. M. *J. Chem. Phys.* **1978**, *68*, 608.
(25) Bowman, J. M. *Acc. Chem. Res.* **1986**, *19*, 202.
(26) Gerber, R. B.; Ratner, M. A. *Adv. Chem. Phys.* **1988**, *70*, 97.
(27) Bowman, J. M.; Christoffel, K.; Tobin, F. *J. Phys. Chem.* **1979**, *83*, 905.
(28) Christoffel, K.; Bowman, J. M. *Chem. Phys. Lett.* **1982**, *85*, 220.
(29) Carter, S.; Bowman, J. M.; Handy, N. C. *Theor. Chem. Acc.* **1998**, *100*, 191.
(30) Christiansen, O. *J. Chem. Phys.* **2004**, *120*, 2149.
(31) Christiansen, O. *Chem. Phys. Phys. Chem* **2007**, *9*, 2942.
(32) Hill, T. L. *An Introduction to Statistical Thermodynamics*, Dover Publications, 1986.
(33) Njegic, B.; Gordon, M. S. *J. Chem. Phys.* **2006**, *125*, 224102.
(34) Chakraborty, A.; Truhlar, D. G. *J. Chem. Phys.* **2006**, *124*, 184310.
(35) Hansen, M. B.; Christiansen, O.; Toffoli, D.; Kongsted, J. *J. Chem. Phys.* **2008**, *128*, 174106.
(36) Becke, A. D. *J. Chem. Phys.* **1993**, *98*, 5648.
(37) Lee, C.; Yang, W.; Parr, R. G. *Phys. Rev. B* **1988**, *37*, 785.
(38) DALTON, an ab initio electronic structure program, Release 2.0, http://www.kjemi.uio.no/software/dalton/dalton.html, 2006.
(39) Jensen, F. *J. Chem. Theory Comput.* **2006**, *2*, 1360.
(40) Jensen, F. *J. Chem. Phys.* **2001**, *115*, 9113.
(41) Huzinaga, S. *J. Chem. Phys.* **1965**, *42*, 1293.
(42) Lutnæs, O. B.; Ruden, T. A.; Helgaker, T. *Magn. Reson. Chem.* **2004**, *42*, 117.
(43) Ruden, T. A.; Helgaker, T.; Jaszuński, M. *Chem. Phys.* **2004**, *296*, 53.
(44) Pecul, M.; Ruud, K. *Magn. Reson. Chem.* **2004**, *42*, 128.
(45) Kutzelnigg, W.; Fleisher, U.; Schindler, M. NMR Basic Principles and Progress; Springer, Berlin, 1990; Vol. 23, p 165.
(46) Kern, C. W.; Matcha, R. L. *J. Chem. Phys.* **1968**, *49*, 2081.
(47) Seidler, P.; Hansen, M. B.; Christiansen, O. *J. Chem. Phys.* **2008**, *128*, 154113.
(48) Malkin, V.; Malkina, O.; Salahub, D. *Chem. Phys. Lett.* **1994**, *221*, 91.
(49) Malkina, O.; Salahub, D.; Malkin, V. *J. Chem. Phys.* **1996**, *105*, 8793.
(50) Lantto, P.; Vaara, J.; Helgaker, T. *J. Chem. Phys.* **2002**, *117*, 5998.
(51) Keal, T. W.; Tozer, D. J.; Helgaker, T. *Chem. Phys. Lett.* **2004**, *391*, 374.
(52) Keal, T. W.; Helgaker, T.; Sałek, P.; Tozer, D. J. *Chem. Phys. Lett.* **2006**, *425*, 163.
(53) Auer, A. A.; Gauss, J. *J. Chem. Phys.* **2001**, *115*, 1619.
(54) Enevoldsen, T.; Oddershede, J.; Sauer, S. P. A. *Theor. Chim. Acta* **1998**, *100*, 275.
(55) Wigglesworth, R. D.; Raynes, W. T.; Kirpekar, S.; Oddershede, J.; Sauer, S. P. A. *J. Chem. Phys.* **2000**, *112*, 3735.
(56) Bass, S. M.; DeLeon, R. L.; Muenter, J. S. *J. Chem. Phys.* **1987**, *86*, 4305.
(57) Wasylishen, R. E.; Friedrich, J. O.; Mooibroek, S. *J. Chem. Phys.* **1985**, *83*, 548.
(58) Friedrich, J. O.; Wasylishen, R. E. *J. Chem. Phys.* **1985**, *83*, 3707.
(59) Sergeyev, N. M.; Sergeyeva, N. D.; Strelenko, Y. A.; Raynes, W. T. *Chem. Phys. Lett.* **1997**, *277*, 144.
(60) Holmes, J. R.; Kivelson, D.; Drinkard, W. C. *J. Chem. Phys.* **1962**, *37*, 150.
(61) Dombi, G.; Diehl, P.; Lounila, J.; Wasser, R. *Org. Magn. Reson.* **1984**, *22*, 573.
(62) Bennett, B.; Raynes, W. T.; Anderson, W. *Spectrochim. Acta, Part A* **1989**, *45*, 821.
(63) Jackowski, K.; Wilczek, M.; Pecul, M.; Sadlej, J. *J. Phys. Chem. A* **2000**, *104*, 5955.

JP804306S